Available online at www.sciencedirect.com
ScienceDirect
Powder Technology 178 (2007) 129–141
POWDER TECHNOLOGY
www.elsevier.com/locate/powtec

On the unsteady forces during the motion of a sedimenting particle

Y.D. Sobral [1], T.F. Oliveira, F.R. Cunha *

Departamento de Engenharia Mecânica, Faculdade de Tecnologia, Universidade de Brasília, Campus Universitário Darcy Ribeiro, 70910-900 Brasília-DF, Brazil

Received 31 March 2006; received in revised form 26 April 2007
Available online 3 May 2007

Abstract

We consider the unsteady motion of a sedimenting rigid spherical particle in order to examine the relative strength of the hydrodynamical forces acting on particles in fluid flows. The relative strength of the forces on all stages of the particle motion is a major concern for closing constitutive equations describing the more complex motion of particulate flows such as fluidised beds. The formulation results in a first order nonlinear integro-differential equation in terms of the instantaneous velocity of the sphere. This equation is made dimensionless and the particle Reynolds number and the fluid–particle density ratio are identified as the relevant physical parameters describing the particle motion. We obtain analytical solutions for the limits of small density ratios and small Reynolds number. In addition, a numerical solution is used for arbitrary values of the density ratio. The results show that the motion of spherical particles is significantly affected by the unsteady drag dominated by the memory Basset force on the early stages of the motion and on the approach to the steady state (terminal velocity). The present calculations indicate that the unsteady hydrodynamic drags might become of the same order of magnitude of the dominant viscous drag for flows with moderate particle–fluid density ratio. Therefore, unsteady drags should be taken into account on modelling multiphase particulate flows with moderate density ratio.

Keywords: Sedimentation; Hydrodynamic drag; Virtual mass; Basset force; Oseen correction

1. Introduction

The correct prediction of the dynamics of particulate flows is of major importance in fluid mechanics. In general, this problem involves several particles with non-negligible inertia in flows in which there is an important relative velocity between the fluid and the particles, and therefore must be treated as two-fluids problem, for which there is an interaction force term that needs to be modelled (e.g. [1–3]). This force represents the interactions between the fluid and the set of particles that compose the particulate flow. A more comprehensive model for this term should consider the full physical mechanisms of interaction between the ambient fluid and the set of particles. In this work, we investigate the motion of one isolated particle sedimentating in a fluid in order to identify and evaluate the relevant mechanisms of interactions that should be considered in continuum models of particulate flows.

G.G. Stokes [4] addressed the motion of an isolated sedimenting particle in a fluid for the case where the inertia of the flow is negligible, the flow field being totally dominated by viscous diffusion. This assumption, however, fails in the regions far from the particle, even for very slow motions, as shown by Oseen [5]. When small amounts of inertia are considered in the region far from the particle by the means of Oseen's approximation, the solution of the flow field is no longer symmetrical, and a wake region, where advection of vorticity becomes an important transport mechanism, is observed. As a result, a small nonlinear correction is obtained for the total drag on the particle.

Basset [6], on the other hand, found a solution to the linear problem, with the non-linear terms of the Navier–Stokes equation being neglected. Basset identified a memory-like contribution to the drag on a particle, which depends on the history of the motion of the particle and on the viscosity of the fluid. This represents a coupling of the inertial and diffusive mechanisms, which are responsible for changing the transport of vorticity in

* Corresponding author. Tel.: +55 61 33072314x229.
E-mail addresses: Y.D.Sobral@damtp.cam.ac.uk (Y.D. Sobral), taygoara@unb.br (T.F. Oliveira), frcunha@unb.br (F.R. Cunha).
[1] Present address: Department of Applied Mathematics and Theoretical Physics, University of Cambridge. Centre for Mathematical Sciences, Wilberforce Road, Cambridge, CB3 0WA, United Kingdom.

0032-5910/$ - see front matter © 2007 Elsevier B.V. All rights reserved.
doi:10.1016/j.powtec.2007.04.012

the flow. In fact, the inertia of the flow is responsible for significant changes in the evolution of the motion of the particle and therefore several studies aim to understand the influence of the Basset memory-force on the motion of particles in several kinds of particulate flows (e.g. [7,8]). Nevertheless, as a consequence of the nonlinearity of the Navier–Stokes equation, the coupling of the nonlinear inertial effects on the wakes of the particles with the transient history-dependent diffusion of vorticity is not simply additive [9]. In fact, one of the most important features of the coupling between the memory force and the Oseen drag is that the decay of the resultant force acting on the particle when it approaches the steady state changes from $t^{-1/2}$ to t^{-2}.

Some works have been concerned with analytical solutions of the equations of motion and whether such solutions are able to reproduce the change in the temporal decay of the resultant force on the particle. Proudman and Pearson [10], and the later extension by Sano [11] obtained an elegant $\mathcal{O}(Re^2\ \ln(Re))$ solution for the drag acting on a spherical particle based on a multi-scale asymptotic analysis of the impulsive motion of the particle and these solution revealed the change of order in time mentioned above. Lovalenti and Brady [9] treated the same problem using the reciprocity theorem [12] to solve directly for the force acting on the particle and obtained several orders of decay in time, such as t^{-1}, $t^{-5/2}\exp(-t)$, $t^{-2}\exp(-t)$, as well as $t^{-1/2}$ and t^{-2}, depending on the initial conditions of the problem. Lawrence and Mei [13] were concerned with the long-time behaviour of impulsive motions of particles in fluids. In their work, they have used a modified convolution kernel for the history-dependent drag on the particle in order to be able to obtain the correct temporal decays of the resultant force acting on the particle.

Maxey and Riley [14] carried out a complete analysis of the motion of a sphere in unsteady Stokes flow for nonuniform flow fields and produced a governing equation for the relative velocity of the particle for any given nonuniform transient background flow, including also terms associated with relative accelerations and Faxén's correction. Coimbra and Rangel [15] have obtained a general solution of the equation of motion for the limit of infinitesimal Reynolds number and uniform background flow. It should be noted that the equation of motion in this case is linear, since the substantial derivatives arising from the far-stream flow are reduced to particle derivatives in time. By solving the problem for a generic background flow field, Coimbra and Rangel [15] applied a linear, multi-scale fractional order operator to convert the fractional differential equation into a linear ordinary differential equation with constant coefficients, but with an extra inhomogeneous term. The use of Riemann–Liouville fractional derivatives allowed the authors to obtain a closed-form solution for the velocity of the particle. Although their results did not recover the expected order of the temporal decay of the resultant force on the particle, it showed that the use of the traditional kernel has little effect on the velocity and particle position at long times.

Many other aspects of fluid flows with particles, and its influence on the dynamics of the particle motion, are also of interest. Thomas and Walters [16] for example, showed that the presence of elasticity in the surrounding fluid increases the velocity sedimentation of spheres, even though the time taken to reach the terminal velocity is unaffected. There are also recent works on the motion of nano-particles, where the non-slip boundary condition does not seem to apply (eg. [17]), therefore changing the nature of some of the forces acting on the particle.

The aim of the present work is three-fold. Firstly, we want to use a simple model for the motion of the particle and obtain analytical and numerical solutions for all limiting regimes of the flow that are consistent with the model. Secondly, based on this simple model, we investigate the time evolution of the particle motion towards the steady state in order to determine which are the relevant forces acting on the particle and in which stages of the particle motion they are relevant. This may indicate the relevant forces that should be considered in modelling the fluid–particle interaction force in continuum formulations of particulate flow problems. Finally, we study the coupling of the inertial and the history-dependent drags in order to determine whether the model explored here is able to reproduce the temporal decays observed in experimental studies of the unsteady hydrodynamic force exerted on an isolated sedimenting particle.

2. The governing equation

The equation of motion of the particle is obtained from Newton's second law, that is

$$\sum \mathbf{F} = m_{\mathrm{p}} \frac{\mathrm{d}\hat{\mathbf{v}}}{\mathrm{d}\hat{t}}, \tag{1}$$

where $\mathbf{F}$ denotes the forces that are acting on the particle, m_{p} is the mass of the particle and $\mathrm{d}\hat{\mathbf{v}}/\mathrm{d}\hat{t}$ its acceleration. Therefore, it is necessary to identify the hydrodynamic and non-hydrodynamic forces acting on the particle in order to solve Eq. (1). Some of the forces are modelled based on scaling arguments of the dimensional Navier–Stokes equation for an incompressible fluid flow, namely

$$\rho_f \left(\frac{\partial \hat{\mathbf{u}}}{\partial \hat{t}} + \hat{\mathbf{u}} \cdot \nabla \hat{\mathbf{u}} \right) = -\nabla \hat{p} + \mu_f \nabla^2 \hat{\mathbf{u}} + \rho_f \mathbf{g}, \tag{2}$$

where $\hat{\mathbf{u}}$ is the fluid velocity, ρ_f and μ_f denote the fluid density and the dynamical viscosity, respectively, $\tilde{p}$ is the pressure on the fluid and $\mathbf{g}$ is the local gravitational acceleration.

Balancing the pressure and the viscous terms in Eq. (2), one observes that there should be a force f_μ, linear in terms of the particle velocity, that scales like $f_\mu \sim \mu_f L U$, where L and U are scales for length and velocity of the particle, respectively. If the nonlinear inertial term is balanced with the pressure term instead, then there should also be a force f_ρ that scales as $f_\rho \sim \rho_f L^2 U^2$, which is found to be nonlinear in terms of the particle velocity. Repeating the same procedure with the transient inertial term, a force $f_{\mathrm{vm}} \sim \rho_f L^3 U/\tau_p$ is found to depend upon a time scale τ_p, denoting the typical time-scale of the particle motion.

In addition to the hydrodynamic forces discussed above, the force corresponding to the net weight of the particle is expressed by

$$\mathbf{f}_g = \vartheta_p(\rho_p - \rho_f)\mathbf{g} = \vartheta_p \Delta\rho \mathbf{g}, \tag{3}$$

which is the force that actually drives the particle motion. In Eq. (3), ϑ_p denotes the volume of the particle and ρ_p represents its density. We also consider a "memory-like" force, the Basset drag $\mathbf{f}_b$, that will be discussed later. Therefore, the equation of motion of a spherical particle in sedimentation can be written as

$$\mathbf{f}_\mu + \mathbf{f}_\rho + \mathbf{f}_{\mathrm{vm}} + \mathbf{f}_b + \mathbf{f}_g = m_p \frac{\mathrm{d}\hat{\mathbf{v}}}{\mathrm{d}\hat{t}}, \tag{4}$$

where all the terms on the left hand side on Eq. (4) are vectorial quantities. Despite the fact that the scales of some of these forces are known, precise relations for each of them need to be proposed.

An expression for the force f_μ can be obtained from the analytical solution of Eq. (2) when the inertia of the flow (both the transient and the convective inertia) is completely neglected and only viscous diffusion of vorticity governs the motion of the fluid. This corresponds to the well know Stokes' solution for viscous drag force [18] of the flow past a sphere given by

$$\mathbf{f}_\mu = 6\pi\mu_f a\hat{\mathbf{v}}, \tag{5}$$

where $\hat{\mathbf{v}}$ is the instantaneous velocity of the particle. When the drag obtained in Eq. (5) is balanced with the net weight of the particle, the terminal velocity, U_s, of the particle is obtained to be

$$U_s = \frac{2}{9}\frac{a^2\Delta\rho \mathrm{g}}{\mu_f}. \tag{6}$$

It is important to note that neglecting the transient part of the flow inertia does not imply that the flow is steady. It means that the forces on the fluid are in dynamical equilibrium, this equilibrium happening in a time-scale much shorter than the time in which the particle motion is developed. Therefore, the instantaneous structure of the flow depends on the boundary conditions of the problem only. In this case, the flow (and the force acting on the particle) is said to be quasi-steady.

Stokes' solution, however, exhibits physical inconsistence in the region far from the sphere, when the inertia of the flow is very small, but not negligible. Now, the scale of the velocity induced on the flow by the motion of the particle at a distance r from its centre is $U_r \sim U_t a/r$, where U_t denotes the terminal velocity of the particle for a Reynolds number not necessarily zero. From Eq. (2), it is obtained that the viscous terms scale as $|\mu_f \nabla^2 \hat{\mathbf{u}}| \sim \mu_f U_t a/r^3$. Far from the particle, the transient inertial term $\partial\hat{\mathbf{u}}/\partial\hat{t}$ in Eq. (2) can be identified with $-\hat{\mathbf{v}}\cdot\nabla\hat{\mathbf{u}}$. This term scales as $|\rho_f \hat{\mathbf{v}}\cdot\nabla\hat{\mathbf{u}}| \sim \rho_f a U_t^2/r^2$, and taking the ratio between this scale and the scale for the viscous terms, its is verified that inertia can be neglected on the flow when $Re_* r/a \ll 1$, where $Re_* = \rho_f a U_t/\mu_f$. Therefore, in the region far from the sphere, $r > a/Re_*$, the Stokes' approximation is no longer valid and inertia cannot be neglected. The Oseen approximation [5] leads to a problem that can be solved analytically for small Re_* limits. The solution to the drag acting on the particle has, besides the linear Stokes drag, a small nonlinear correction that we identify as being $\mathbf{f}_\rho$, that is,

$$\mathbf{f}_p = \frac{9}{4}\pi a^2 \rho_f \hat{\mathbf{v}}|\hat{\mathbf{v}}|. \tag{7}$$

The unsteady force $\mathbf{f}_{\mathrm{vm}}$ is associated to the inertia of the fluid surrounding the particle. This is called the virtual mass drag and can be calculated from the potential flow past a sphere [18], namely

$$\mathbf{f}_{\mathrm{vm}} = \frac{2}{3}\pi a^3 \rho_f \frac{\mathrm{d}\hat{\mathbf{v}}}{\mathrm{d}\hat{t}}. \tag{8}$$

Note that the coefficient of the time derivative in Eq. (8) is the mass of fluid associated with half of the volume of the sphere, corresponding to the mass of fluid accelerated by the particle.

Now, we give the expression for the force $\mathbf{f}_b$. Basset [6] developed an analytical solution of Eq. (2) for the case in which the nonlinear term $\rho_f \hat{\mathbf{u}}\cdot\nabla\hat{\mathbf{u}}$ is neglected. This problem can be solved by the means of spherical harmonics or by Fourier transform [19], and the solution to the hydrodynamic force on the sphere yields the Stokes drag, the virtual mass drag and an extra unsteady force given by the following convolution integral

$$\mathbf{f}_b = 6a^2\sqrt{\pi\rho_f\mu_f}\int_o^{\hat{t}} \left(\frac{\mathrm{d}\hat{\mathbf{v}}}{\mathrm{d}\hat{t}}\right)_{\hat{t}=\hat{\zeta}} \frac{1}{\sqrt{\hat{t}-\hat{\zeta}}}\mathrm{d}\hat{\zeta}, \tag{9}$$

where $\hat{\zeta}$ is an integration variable. This term couples the history of the acceleration of the particle with the viscosity of the fluid, indicating a transient diffusion of vorticity in the flow. In fact, the coefficients of the Basset force in Eq. (9) may be re-written in terms of the Stokes drag coefficient, in Eq. (5), and that of the virtual mass drag in Eq. (8), as follows:

$$a^2\sqrt{\rho_f\mu_f} = \sqrt{(\mu_f a)(\rho_f a^3)}. \tag{10}$$

So, the coefficient of the Basset force corresponds to the geometric mean of the viscous drag coefficient and the virtual mass drag coefficient.

Now, we consider the 1D version of Eq. (4) adopting the positive sense of motion downwards. By this convention, the drag forces that resist the motion of the particle are negative forces. We obtain

$$\begin{aligned} m_p\frac{\mathrm{d}\hat{\mathrm{v}}}{\mathrm{d}\hat{t}} = &-6\pi\mu_f a\hat{\mathrm{v}} - \frac{9}{4}\pi\rho_f a^2\hat{\mathrm{v}}^2 - \frac{2}{3}\pi\rho_f a^3\frac{\mathrm{d}\hat{\mathrm{v}}}{\mathrm{d}\hat{t}} \\ &-6a^2\sqrt{\pi\rho_f\mu_f}\int_o^{\hat{t}}\left(\frac{\mathrm{d}\hat{\mathrm{v}}}{\mathrm{d}\hat{t}}\right)_{\hat{t}=\hat{\zeta}}\frac{1}{\sqrt{\hat{t}-\hat{\zeta}}}\mathrm{d}\hat{\zeta} \\ &+\vartheta_p(\rho_p-\rho_f)\mathrm{g}, \end{aligned} \tag{11}$$

where $\hat{\mathrm{v}}$ is the dimensional 1D particle velocity and g is the acceleration of gravity.

Eq. (11) can be made nondimensional by choosing the terminal Stokes velocity U_s in Eq. (6) and the particle relaxation time, $\tau_r = m_p/(6\pi\mu_f a)$, as the characteristic velocity and time scales,

respectively. Defining the dimensionless variables $v=\hat{v}/U_s$ and $t=\hat{t}/\tau_r$, Eq. (11) can be written in a nondimensional form as

$$\left(1+\frac{1}{2}\chi\right)\frac{dv}{dt}+v+\frac{3}{8}Re_s v^2 + \sqrt{\frac{9\chi}{2\pi}}\int_o^t \left(\frac{dv}{dt}\right)_{t=\zeta}\frac{1}{\sqrt{t-\zeta}}d\zeta - 1 = 0. \quad (12)$$

In the above equation, two relevant physical parameters governing the particle motion are identified: the density ratio $\chi=\rho_f/\rho_p$ and the Reynolds number based on the Stokes terminal velocity, $Re_s=\rho_f a U_s/\mu_f$. It should be noted that if the terminal velocity of the particle U_t had been chosen as a velocity scale, instead of U_s, we would find, in addition to the Reynolds number and the density ratio, the sedimentation number $N_s=U_s/U_t$ (note that for the Stokes regime, $U_t=U_s$ and $N_s=1$). Eq. (12) is an integro-differential nonlinear first-order differential equation and is associated to the initial condition

$$v(0)=0. \quad (13)$$

The solution of Eqs. (12) and (13) gives the velocity of the particle as a function of time. As we will discuss later, an analytical solution of Eq. (12) in its complete form has not yet been obtained. Some particular cases, however, can be solved analytically, allowing a precise analysis of each individual mechanism (or force) that was incorporated to the present model.

3. Analytical solutions of the governing equation

3.1. Linear equation without memory effects

This is the simplest form of Eq. (12), corresponding to the case in which only the viscous and the virtual mass forces are considered in addition to the net weight of the particles. In this case, Eq. (12) reduces to

$$\left(1+\frac{1}{2}\chi\right)\frac{dv}{dt}+v-1=0, \quad (14)$$

that admits direct integration. For this simple case the velocity of the particle is simply given by

$$v(t)=1-\exp\left(-\frac{t}{1+\frac{1}{2}\chi}\right). \quad (15)$$

3.2. Nonlinear equation without memory effects

When only the memory effects are neglected in Eq. (12), the motion of the particle is governed by the following nonlinear inhomogeneous differential equation

$$\left(1+\frac{1}{2}\chi\right)\frac{dv}{dt}+v+\frac{3}{8}Re_s v^2-1=0. \quad (16)$$

The first information about the motion of the particle that can be obtained from this equation is its terminal velocity as a function of the parameter Re_s. This can be determined analytically from Eq. (16), since when the particle reaches the terminal velocity its acceleration vanishes. Then:

$$-v_t-\frac{3}{8}Re_s v_t^2+1=0, \quad (17)$$

where $v_t=U_t/U_s$ denotes the terminal dimensionless velocity of the particle, and therefore:

$$v_t=\frac{-8+\sqrt{64+96Re_s}}{6Re_s}. \quad (18)$$

Note that only the solution corresponding to $v_t>0$ in Eq. (18) is considered. In addition, from Eq. (17), note that for $Re_s\to 0$, $v_t\to 1$.

Eq. (16) is a Ricatti equation (with constant coefficients) and an analytical solution to it can be found using the well-known transformation:

$$v=v^*+\frac{1}{u}, \quad (19)$$

provided a particular solution v^* of Eq. (16) is known. The function u is a function of time that has be found.

Defining $\varepsilon=\frac{3}{8}Re_s$, and applying the transformation in Eq. (19) to Eq. (16), and noting that Eq. (18) is, in fact, a particular solution of Eq. (16), we obtain that u has to satisfy the following equation:

$$\mathcal{A}\frac{du}{dt}-(2\varepsilon v_t+1)u=\varepsilon, \quad (20)$$

with

$$\mathcal{A}=1+\frac{1}{2}\chi, \quad (21)$$

and with initial condition $u(0)=-1/v_t$. Eq. (20) can be solved for u using an integration factor and, substituting the solution of this equation into Eq. (19), the solution $v(t)$ to Eq. (16) is obtained as:

$$v(t)=v_t\left\{1+\frac{1+2\varepsilon v_t}{(1-\varepsilon v_t)\exp[(1+2\varepsilon v_t)t/\mathcal{A}]-\varepsilon v_t}\right\}. \quad (22)$$

Note that it is also possible to solve Eq. (16) by separation of variables and manipulating the equation to get a hyperbolic tangent solution or simply using partial fractions, since all the coefficients are constant.

As a complementary calculation, it is instructive to obtain an asymptotic solution when Eq. (16) is weakly nonlinear, that is, for small values of the parameter ε defined above. The solution of Eq. (16) can be proposed in terms of an asymptotic expansion

for $v(t)$. We then found the asymptotic solution for the velocity of the particle up to the $\mathcal{O}(\varepsilon^4)$ terms as

$$v(t) = v_o(t) + \varepsilon v_1(t) + \varepsilon^2 v_2(t) + \varepsilon^3 v_3(t) + \varepsilon^4 v_4(t) + O(\varepsilon^5). \tag{23}$$

with

$$v_o(t) = 1 - \exp\left(-\frac{t}{\mathcal{A}}\right), \tag{24}$$

$$v_1(t) = -1 + \frac{2t}{\mathcal{A}}(1 - v_o(t)) + (1 - v_o(t))^2, \tag{25}$$

$$v_2(t) = 2 + \left(1 - \frac{2t}{\mathcal{A}} - \frac{2t^2}{\mathcal{A}^2}\right)(1 - v_o(t)) - 2\left(1 + \frac{2t}{\mathcal{A}}\right)(1 - v_o(t))^2 - (1 - v_o(t))^3, \tag{26}$$

$$v_3(t) = -5 + \left(-4 + \frac{2t}{\mathcal{A}} + \frac{4t^2}{\mathcal{A}_2} + \frac{4}{3}\frac{t^3}{\mathcal{A}_3}\right)(1 - v_o(t)) + 4\left(1 + \frac{3t}{\mathcal{A}} + \frac{2t^2}{\mathcal{A}^2}\right) \times (1 - v_o(t))^2 + 2\left(2 + \frac{3t}{\mathcal{A}}\right)(1 - v_o(t))^3 + (1 - v_o(t))^4, \tag{27}$$

$$v_4(t) = 14 + \left(14 - \frac{8t^2}{\mathcal{A}_2} - \frac{4t^3}{\mathcal{A}_3} - \frac{2}{3}\frac{t^4}{\mathcal{A}_4}\right)(1 - v_o(t)) - 8\left(1 + \frac{4t}{\mathcal{A}} + \frac{4t^2}{\mathcal{A}_2} + \frac{4t^3}{\mathcal{A}_3}\right) \times (1 - v_o(t))^2 - \left(13 + \frac{30t}{\mathcal{A}} + \frac{18t^2}{\mathcal{A}_2}\right)(1 - v_o(t))^3 - 2\left(3 + \frac{4t}{\mathcal{A}}\right) \times (1 - v_o(t))^4 - (1 - v_o(t))^5. \tag{28}$$

It is important to note that the $\mathcal{O}(1)$ leading order term, v_o, is the solution of Eq. (16) for the case of zero particle Reynolds number, $Re_s = 0$, that is, the solution discussed in Section 3.1. The nonlinear effects are brought to the solution by the higher order terms in ε. The solution given in Eqs. (23), (24), (25), (26), (27), and (28) show the nonlinear contribution related to the Oseen correction for moderate values of $Re_s = \mathcal{O}(1)$.

Fig. 1 shows the results for the terminal velocity of the particle given by the asymptotic solution in Eq. (23) and Eq. (18), as a function of Re_s. The terminal velocity of the particle decreases as Re_s increases due to the increase of the total drag acting on the particle. Consequently, the resistance to the particle motion increases due to the presence of inertial effects in a regime of non-zero particle Reynolds number. The $\mathcal{O}(1)$ solution shows that the particle sediments with a terminal velocity independent of Re_s. This result is not verified by experimental observations for finite Reynolds numbers. As the higher order terms are considered in the asymptotic solution a better agreement of the particle terminal velocity is observed. The maximum value of Re_s for which a good agreement (with an error less than 2%) is still observed when comparing the $\mathcal{O}(\varepsilon^4)$ solution with Eq. (18) is $Re_s = 1/2$. It should be stressed that Oseen's correction is valid for $Re_s = \mathcal{O}(1)$ and, if larger values of Re_s are used, the Oseen approximation produces physically inconsistent results.

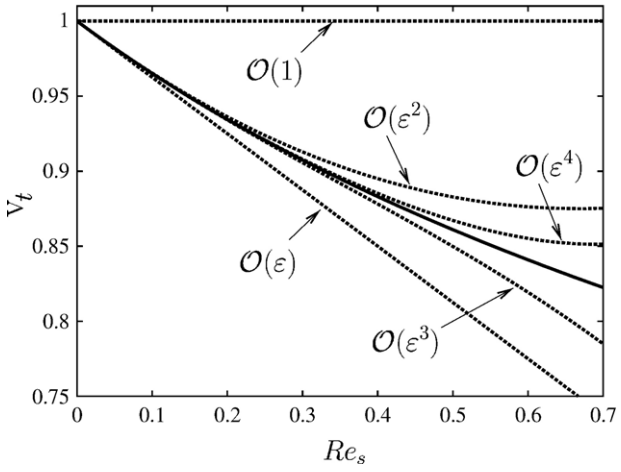

Fig. 1. Terminal velocity of the particle as a function of Re_s. The solid line represents the predictions given by Eq. (18) and the dotted lines represent the asymptotic solutions expressed by Eq. (23), up to the order indicated on the figure.

3.3. Linear equation with memory effects

In this case, the inertial nonlinear drag in Eq. (12) is not considered. So, Eq. (12) reduces to the following integro-differential equation

$$\left(1 + \frac{1}{2}\chi\right)\frac{dv}{dt} + v + \sqrt{\frac{9\chi}{2\pi}}\int_o^t \left(\frac{dv}{dt}\right)_{t=\zeta} \frac{1}{\sqrt{t-\zeta}}d\zeta - 1 = 0. \tag{29}$$

This equation can be solved analytically by different means, by the use of the Abel transformation [20] or by Laplace transforms [16], for example. In this work, we adopted the last procedure and used the Laplace transform as defined in Abramowitz and Stegun [21]. For the initial condition $v(0) = 0$, and using $\mathcal{A}$ as defined in Eq. (21) and $\mathcal{B} = (9\chi/2\pi)^{1/2}$ the following algebraic equation is obtained in terms of the Laplace transform of the particle velocity $\tilde{v}$:

$$\mathcal{A}s\tilde{v} + \tilde{v} + \mathcal{B}(s\tilde{v})\left(\sqrt{\frac{\pi}{\sqrt{s}}}\right) - \frac{1}{s} = 0. \tag{30}$$

Solving Eq. (30) for $\tilde{v}$ and making few algebraic manipulations, we obtain

$$\tilde{v} = \frac{\mathcal{A}s + 1 - \mathcal{B}\sqrt{\pi s}}{s\left[(\mathcal{A}s+1)^2 - \mathcal{B}^2\pi s\right]}. \tag{31}$$

Now, using inverse Laplace transform tables available in Abramowitz and Stegun [21] and the software Maple 7 to perform this calculation, Eq. (31) is inverted to give the velocity of the particle as a function of time

$$v(t) = 1 + \mathcal{C}_1(\exp(\mathcal{C}_2 t) - \exp(\mathcal{C}_3 t)) - \exp(\mathcal{C}_4 t)(\cosh(\mathcal{C}_5 t) + \mathcal{C}_6 \sinh(\mathcal{C}_5 t)) + \mathcal{C}_7 \mathrm{erf}(\mathcal{C}_8\sqrt{t})\exp(\mathcal{C}_9 t) - \mathcal{C}_{10}\mathrm{erf}(\mathcal{C}_{11}\sqrt{t})\exp(\mathcal{C}_{12} t), \tag{32}$$

where erf is the error function and the coefficients $\mathcal{C}_1 \ldots \mathcal{C}_{12}$ are given as follows

$$\mathcal{C}_1 = \frac{\mathcal{A}}{\sqrt{-\mathcal{B}^2\pi(-\mathcal{B}^2\pi + 4\mathcal{A})}} \tag{33}$$

$$\mathcal{C}_2 = -\frac{2\mathcal{A} - \mathcal{B}^2\pi - \sqrt{\mathcal{B}^4\pi^2 - 4\mathcal{A}\mathcal{B}^2\pi}}{2\mathcal{A}^2} \tag{34}$$

$$\mathcal{C}_3 = -\frac{2\mathcal{A} - \mathcal{B}^2\pi + \sqrt{\mathcal{B}^4\pi^2 - 4\mathcal{A}\mathcal{B}^2\pi}}{2\mathcal{A}^2} \tag{35}$$

$$\mathcal{C}_4 = -\frac{2\mathcal{A} - \mathcal{B}^2\pi}{2\mathcal{A}^2} \tag{36}$$

$$\mathcal{C}_5 = \sqrt{\frac{\mathcal{B}^4\pi^2 - 4\mathcal{A}\mathcal{B}^2\pi}{2\mathcal{A}^2}} \tag{37}$$

$$\mathcal{C}_6 = \frac{2\mathcal{A} - \mathcal{B}^2\pi}{\sqrt{\mathcal{B}^4\pi^2 - 4\mathcal{A}\mathcal{B}^2\pi}} \tag{38}$$

$$\mathcal{C}_7 = \frac{2\mathcal{A}\mathcal{B}\sqrt{\pi}}{\sqrt{-4\mathcal{A} + 2\mathcal{B}^2\pi - 2\sqrt{-4\mathcal{A}\mathcal{B}^2\pi + \mathcal{B}^4\pi^2}}\sqrt{-4\mathcal{A}\mathcal{B}^2\pi + \mathcal{B}^4\pi^2}} \tag{39}$$

$$\mathcal{C}_8 = \sqrt{\frac{-4\mathcal{A} + 2\mathcal{B}^2\pi - 2\sqrt{-4\mathcal{A}\mathcal{B}^2\pi + \mathcal{B}^4\pi^2}}{2\mathcal{A}}} \tag{40}$$

$$\mathcal{C}_9 = \frac{\mathcal{B}^2\pi}{2\mathcal{A}^2} - \frac{1}{\mathcal{A}} - \frac{\sqrt{-4\mathcal{A}\mathcal{B}^2\pi + \mathcal{B}^4\pi^2}}{2\mathcal{A}^2} \tag{41}$$

$$\mathcal{C}_{10} = \frac{2\mathcal{A}\mathcal{B}\sqrt{\pi}}{\sqrt{-4\mathcal{A} + 2\mathcal{B}^2\pi + 2\sqrt{-4\mathcal{A}\mathcal{B}^2\pi + \mathcal{B}^4\pi^2}}\sqrt{-4\mathcal{A}\mathcal{B}^2\pi + \mathcal{B}^4\pi^2}} \tag{42}$$

$$\mathcal{C}_{11} = \sqrt{\frac{-4\mathcal{A} + 2\mathcal{B}^2\pi + 2\sqrt{-4\mathcal{A}\mathcal{B}^2\pi + \mathcal{B}^4\pi^2}}{2\mathcal{A}}} \tag{43}$$

$$\mathcal{C}_{12} = \frac{\mathcal{B}^2\pi}{2\mathcal{A}^2}\frac{1}{\mathcal{A}} + \frac{\sqrt{-4\mathcal{A}\mathcal{B}^2\pi + \mathcal{B}^4\pi^2}}{2\mathcal{A}^2} \tag{44}$$

Despite the fact that we have found an analytical solution for Eq. (29), the error function which appears in Eq. (32) needs to be calculated for complex arguments, and that caused problems on the computations of this function based on the incomplete gamma function (e.g. [22]) . It can be observed that the solution presented in Eq. (32) can be simplified and combined with a thorough analysis of the coefficients presented in Eq. (33)–(44), in such a way that complex terms will cancel out and a final real-only solution could be found. In addition, if the only interest was the long time behaviour of the solution, an asymptotic approximation could have been found, in a similar way as in Belmonte et al. [20]. However, for the scope of the present study, the most appropriate way to deal with this issue was to use the software Maple 7 to evaluate numerically the error function and the large values it may assume.

3.4. Nonlinear equation with memory effects

This case corresponds to the full nonlinear governing equation presented in Eq. (12), to which an analytical solution has not been found yet. In order to solve the full integro-differential Eq. (12), a numerical procedure must be used. A brief description of the algorithm used to solve Eq. (12) is presented below.

Using $B(t)$ to denote the Basset term, tol to denote a numerical tolerance and the superscript n to indicate the iteration number, the Picard algorithm presented in Table 1 was implemented. The evaluation of $v(t)$, necessary in the steps (1.2) and (2.3), was made by using a fourth order Runge–Kutta scheme. Isolating $\mathrm{d}v(t)/\mathrm{d}t$ in Eq. (12), step (2.1) is performed directly. The evaluation of the convolution integral requires more attention. As the kernel of the integral, $(t-\zeta)^{-\frac{1}{2}}$, is singular at $\zeta = t$, it was necessary to subtract the singularity in order to perform the convolution integral at each time step. Details of this procedure can be viewed in the Appendix. The convolution integral was calculated by a trapezoidal rule. It is important to notice that in order to calculate $B(t)$ for each t, an integration from 0 to t must be performed. This approach leads to a procedure with the computational efforts of $\mathcal{O}(N^2)$, where N is the number of time steps in the simulation. More than 90% of the computational time of each iteration is spent in the memory term evaluation. Typically, the time step used in the Runge–Kutta scheme coupled with the trapezoidal rule to solve the memory integral at each time meets the following condition:

$$\Delta t = \frac{1}{5}\min\left\{\chi, \frac{\chi}{Re_s}\right\}. \tag{45}$$

With this time we ensure that the position of the particle changed little in one time step. For moderate density ratios χ,

Table 1
Picard algorithm to solve Eq. (12)

(1) For $n=1$
  (1.1) $B^n(t) \leftarrow 0$
  (1.2) Evaluate $v^n(t)$
(2) For $n>1$
  (2.1) Evaluate $\frac{dv^n}{dt}(t)$
  (2.2) Evaluate $B^n(t)$
  (2.3) Evaluate $v^{n+1}(t)$
  (2.4) err $\leftarrow \sum_{i=1}^{N}(v_i^{n+1}-v_i^n)^2$
  (2.5) If err < tol then
    (2.5.1) Evaluate $B^{n+1}(t)$
    (2.5.2) Go to (3)
  (2.6) If err ≥ tol then
    (2.6.1) $v^n \leftarrow v^{n+1}$
    (2.6.2) Go to (2.1)
(3) End

the convergence rate of the Picard method is very slow, and the numerical solution of Eq. (12) was of considerable computational cost. About 70 hours of CPU time were required for an integration over $100\tau_r$, corresponding to a typical numerical computation in the presence of the memory contribution. With the numerical procedure developed here, we have performed computations to investigate the coupling between the memory force and the nonlinear inertial force on the particle motion.

4. Results and discussion

Once the velocity of the particle as a function of time is obtained, it is possible to evaluate the time evolution of each hydrodynamic force acting on the particle. We examine, for different conditions of Re_s and χ, which of the forces are the predominant during the motion of the particle. As stated previously, a phenomenological analysis of the motion of the particle is important to determine the fluid–particle interaction forces that are needed for modelling particulate two-phase flows.

The first result to be analysed refers to the time evolution of the particle presented in Fig. 2 for $\chi=1/100$ and $\chi=1/2$. The values for χ were chosen in order to represent typical situations of fluid suspensions such as a gas–solid fluidised bed, in which $\chi \ll 1$, and a liquid–solid fluidised bed, where χ is typically $\mathcal{O}(1)$, say 1/2. Based on the results presented in Fig. 2, we can

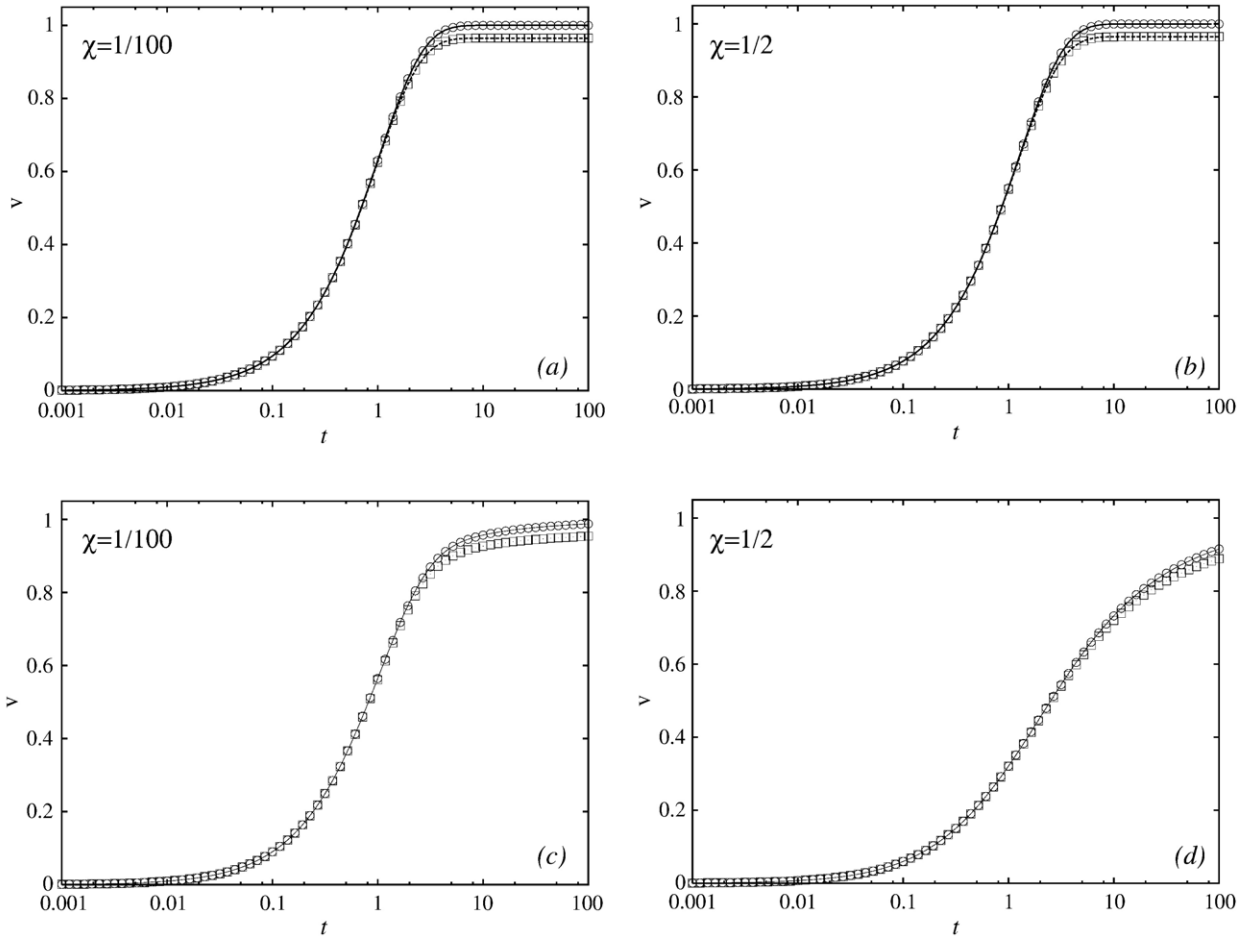

Fig. 2. Time evolution of the particle velocity for $\chi=1/100$ (left, *(a)* and *(c)*) and $\chi=1/2$ (right, *(b)* and *(d)*). In all graphs, solid line denotes the analytical solution of the linear problem ($Re_s=0$) and the dashed lines in graphs *(a)* and *(b)* represent the analytical solution for the nonlinear problem without memory effects for $Re_s=1/10$. In all graphs, ⊙ the represent the numerical solution of the linear problems ($Re_s=0$) and ⊡ represent the numerical solution of the nonlinear problem with memory effects for $Re_s=1/10$.

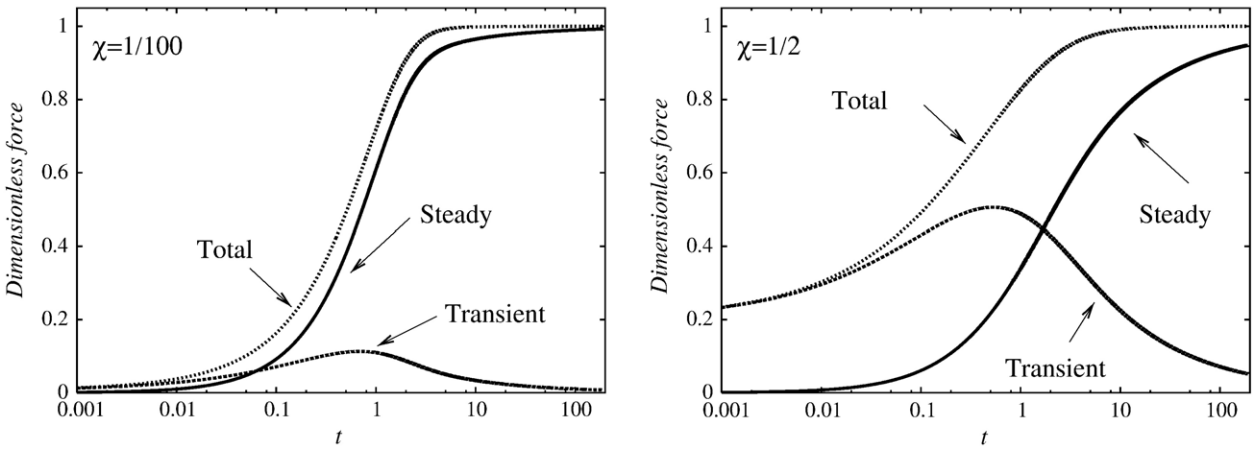

Fig. 3. Time evolution of the hydrodynamic forces acting on the particle, for $\chi = 1/100$ (left) and for $\chi = 1/2$ (right). In both plots, $Re_s = 1/2$. The label "steady" identifies the linear viscous drag and the nonlinear inertial drag, the label "transient" identifies the Basset memory drag and the virtual mass drag and the label "total" represents the total force acting on the particle.

see that the numerical solution of Eq. (12) is in perfect agreement with the analytical solutions for the particular cases studied here. In addition, the results indicate that the transient diffusion of vorticity in the flow has an important influence on the motion of the particle, mainly on its evolution to the steady state at terminal velocity. This effect is noticeable for particles with density of the same order as that of the fluid, that is for $\chi \sim 1$. In this case, the time in which the particle reaches its terminal velocity may change from $\mathcal{O}(1)$ to $\mathcal{O}(100)$, depending whether the memory force is considered or not on the particle motion. For $\chi \ll 1$, however, the time in which the terminal velocity is achieved is $\mathcal{O}(1)$.

On the other hand, the plots in Fig. 2 show that the contribution of the Oseen inertial drag does not change the initial evolution of particle, independently of whether the Basset drag was absent or not. At long times, however, the particle velocity is slightly changed so that the terminal velocity predicted by Eq. (18) is reached smoothly. Nevertheless, it is important to comment that the asymptotic solution for the nonlinear case with no memory effects does reproduce with fidelity, for times of the order of the particle relaxation time, the temporal evolution of the particle velocity, but overestimates the terminal velocity by approximately 2% the value of the terminal velocity for $Re_s = 1/2$. The time in which the terminal velocity is achieved is almost unaffected by the nonlinear drag and is comparable to those obtained in the linear cases. Fig. 2 shows that the Basset force is responsible for the major changes in the time-evolution of particle motion. This means that the flow memory, which is responsible for changing the mechanisms of a transient diffusion of vorticity, causes a significant delay in the evolution of the particle. This mechanism, nevertheless, does not change the terminal velocity of the particle that is predicted by the linear case governed by Eq. (14). The particle will reach its Stokes terminal velocity, although it will happen in a time-scale that is much larger than the one predicted by Eq. (15). For instance, this time scale may even be of the order of the time required by the particle to go through all the sedimentation container in an laboratory experiment, that is, a time scale

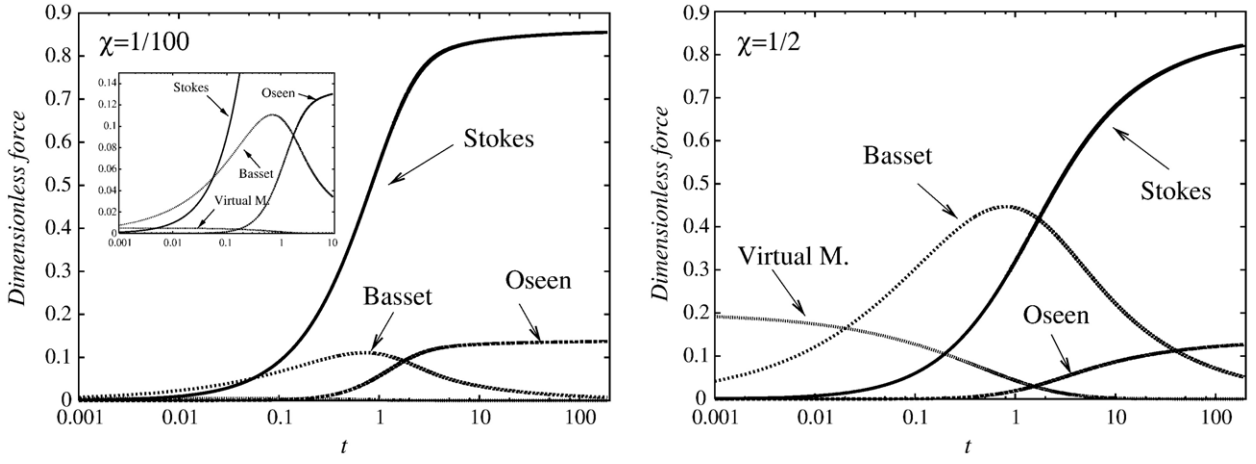

Fig. 4. Time evolution of the forces acting on the particle for $\chi = 1/100$ (left) and for $\chi = 1/2$ (right). In both plots, $Re_s = 1/2$. The insert for $\chi = 1/100$ illustrates the early stages of the particle motion.

$\mathcal{O}(L/U_s)$, with L denoting the length of the container. It is also seen that the relaxation time of the particle increases significantly as χ increases.

The total, transient and permanent hydrodynamic forces acting on the particles are presented in Fig. 3 for $\chi=1/100$ and $\chi=1/2$, and the isolated forces in Fig. 4. We can see that the transient forces are predominant on the early stages of the motion, especially for the case $\chi=1/2$. In this case, both the virtual mass and the Basset drag are more important than the pseudo-steady viscous and inertial drags during the first period of the particle motion, as shown in more detail in Fig. 4. When $\chi=1/100$, a similar behaviour is observed, but is restricted to considerably smaller time-intervals. In fact, the virtual-mass unsteady drag is greater than the viscous Stokes drag during the first 3/500 units of dimensionless time of the motion, whereas the Basset drag is important up to the 1/20 units of dimensionless time. The analysis of the plots in Figs. 3 and 4 suggests that the inertial transients have a negligible contribution in modelling suspensions of particles with much greater inertia than the fluid, that is $\chi \ll 1$ (e.g. dusty gas-suspension). In other words, one would say that the motion of particles in gas–solid suspensions is little influenced by any unsteady drag. This is related to the fact that the amount of kinetic energy of the particle motion used to accelerate the surrounding fluid is very small, and consequently these unsteady hydrodynamic drags decay very rapidly compared with the particle relaxation time.

Fig. 4, for $\chi=1/100$, also shows that the virtual mass contribution is significant only during the first 1/10 units of dimensionless time of the motion of the particle, and that it decays rapidly as the motion evolves. Note that, at this time, the Stokes drag is almost 10 times greater than this force. This result suggests that, for small values of χ, the virtual-mass unsteady force can be neglected with no major consequences to an accurate prediction of particle motion. In contrast, for $\chi=1/2$ the virtual mass force has an important contribution during one relaxation time τ_r. These findings can also be inferred from the solution obtained in Eq. (15), plotted in Fig. 5. It is observed that for $\chi=1/100$, the particle history is approximately the same as the one predicted when the virtual mass force is absent (i.e. making $\chi=0$ in Eq. (15)). On the other hand, the particle takes more time to reach the terminal velocity when $\chi=1/2$, since it was retarded by the strong virtual mass force on the early stages of its motion.

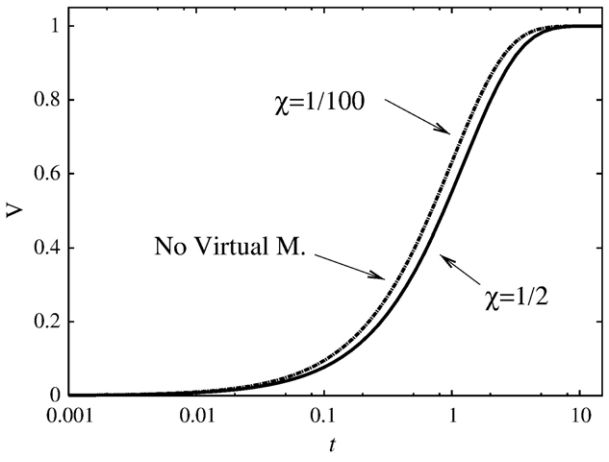

Fig. 5. Influence of the virtual-mass force on the motion of the particle predicted by Eq. (15) for $\chi=1/100$ (dotted line) and $\chi=1/2$ (solid line). The dashed line represents the motion of the particle when the virtual-mass is absent.

Fig. 6 shows simulation results for the particle motion when the unsteady Basset drag and the Oseen drag contribution are considered. We observe that the inertia of the wakes of the particles, brought into the model by the Oseen drag, does not affect significantly the time evolution of the Basset drag, the latter being reduced by about 15% on the interval between the first and the 100th units of dimensionless time, for the case $\chi=1/100$. It is also seen that for the case $\chi=1/2$, this reduction persists for more than 100 units of dimensionless time. In addition, the intensity of the Basset drag was reduced by about 73% when χ was reduced to 1/100, confirming that the inertial unsteady forces lose importance as $\chi \to 0$. In particular, if on one hand the time when the maximum of the Basset force is reached is not sensitive to changes in χ, it is slightly influenced by the convective inertia, on the other hand. For $Re_s=1/2$, the peak of the Basset drag is advanced by 1/10 of unit of dimensionless time, but still remains on the neighbourhood of $t=1$. In fact, the time-scale used to convert the dimensional variables of the problem into dimensionless variables, the particle relaxation time, denotes the scale in which the Basset drag reaches its maximum. Therefore, it is observed that the Basset drag is a force that grows very rapidly, reaches its maximum in the neighbourhood of one particle relaxation time and decays very slowly, as can be seen on Fig. 6 (note the logarithmic scale). This force takes more than 100 units of dimensionless time to decay to the levels of intensity associated to the beginning of the motion (i.e. when $t \sim 10^{-3}$). For this reason, the omission of this force in modelling fluid–particle interactions in two-phase particulate flows where the inertia of the fluid is not negligible may lead to imprecise results in the prediction of the dynamics of the flow. Fig. 6 also presents the influence of the Basset drag on the evolution of the Oseen drag. An important delay in reaching the steady state can be observed. In particular, the unsteady diffusion of vorticity that occurs in the wakes of the particle for distances greater than the Oseen distance, i.e. $r > aRe_s^{-1}$, competes with the convective transport of vorticity in this region and is responsible for reducing its intensity during three units of dimensionless time, for $\chi=1/100$, and about ten units of dimensionless time for $\chi=1/2$. This is directly related to the fact that the vorticity that is created on the particle surface and that is captured by the wake, is both convected by the flow in this region and diffused in the presence of inertial effects. In other words, the diffusive transport of vorticity is affected by the convective transport of vorticity in the region $r \sim aRe_s^{-1}$.

Lovalenti and Brady [9] and Lawrence and Mei [13] have argued that the evolution of the particle to reach its terminal velocity changes its temporal decay from t^{-2} to t^{-2} when convective effects are coupled to the unsteady memory diffusion effects in the description of the sedimentation of a particle starting from rest. More precisely, in Lovalenti and Brady [9], and in its appendix D written by Hinch, different time

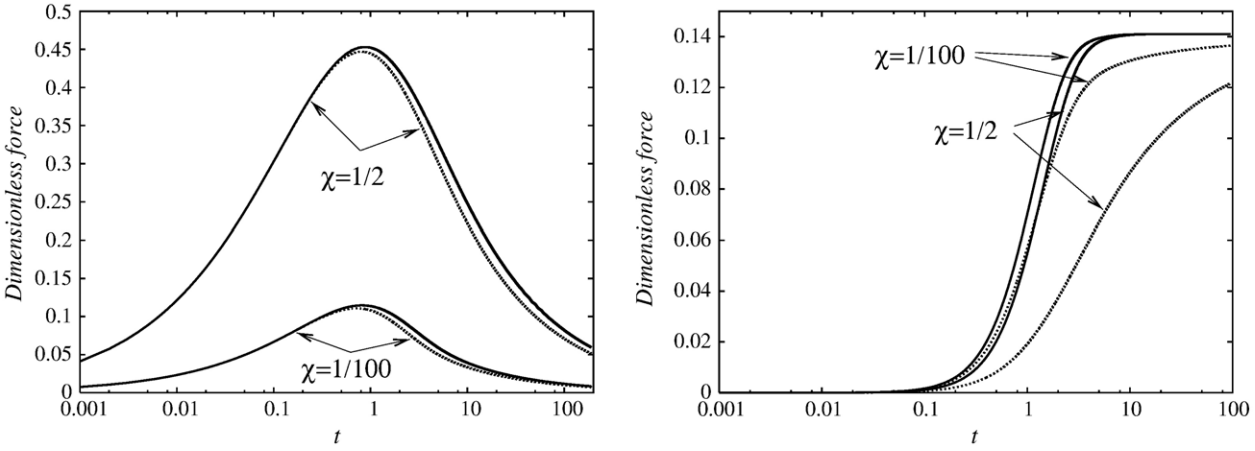

Fig. 6. Left picture: Time evolution of the Basset drag for $\chi=1/2$ and for $\chi=1/100$. Solid lines represent the case with no Oseen drag and dotted lines represent the case with Oseen drag for $Re_s=1/2$. Right picture: Evolution of the Oseen drag for $Re_s=1/2$, for $\chi=1/2$ and $\chi=1/100$. Solid lines denote the case in the absence of Basset drag and dotted lines represent the case as Basset drag is considered.

decays were predicted for several cases of arbitrary motion of a spherical particle. Now, we use scaling arguments in order to derive the time decay law for the total force acting on the particle for the present model. Let us consider the equation of motion in its dimensional version, Eq. (11). A scale for the Basset drag is given by

$$\text{Basset} = 6a^2\sqrt{\pi\rho_f\mu_f}\int_o^{\hat{t}}\left(\frac{\mathrm{d}\hat{\mathbf{v}}}{\mathrm{d}\hat{t}}\right)_{\hat{t}=\hat{\zeta}}\frac{1}{\sqrt{\hat{t}-\hat{\zeta}}}\mathrm{d}\hat{\zeta}\sim a^2\sqrt{\rho_f\mu_f}\frac{U}{t^{\frac{1}{2}}}, \tag{46}$$

where U is a velocity scale and t is a characteristic time scale of the flow. In addition, a scale for the Oseen drag is found to be

$$\text{Oseen} = \frac{9}{4}\pi\rho_f a^2\hat{\mathbf{v}}^2\sim\rho_f a^2U^2. \tag{47}$$

We have identified three different steps in the transient motion of the particle. During the first step, when the particle is starting its motion, the important velocity scale is associated with vorticity diffusion, i.e. $U\sim\nu_f/a$, where ν_f is the kinematic viscosity μ_f/ρ_f. In this case, Eqs. (46) and (47) are rewritten as:

$$\text{Basset}\sim a\rho_f^{-\frac{1}{2}}\mu_f^{\frac{3}{2}}\hat{t}^{-\frac{1}{2}} = \mathcal{O}\left(t^{-\frac{1}{2}}\right), \tag{48}$$

$$\text{Oseen}\sim\mu_f^2\rho_f^{-1} = \mathcal{O}(1). \tag{49}$$

Eqs. (48) and (49) indicate that, at the early stages of the particle motion, the Basset drag evolves temporally as $t^{-\frac{1}{2}}$, whereas the Oseen drag is $\mathcal{O}(1)$ (see Fig. 3). The validity of these scales is restricted to the time-interval defined at the beginning of the motion, that is, for $t\sim 0$ to 1 (or even $t\sim 0$ to 10, for $\chi=\mathcal{O}(1)$).

The second part of the motion is observed close to the steady state, when the particle is reaching its terminal velocity. Under this condition the appropriate velocity scale is simply the convective particle velocity $a/\hat{t}$. With this scale, Eqs. (46) and (47) take the form

$$\text{Basset}\sim a^3\rho_f^{\frac{1}{2}}\mu_f^{\frac{1}{2}}\hat{t}^{-\frac{3}{2}} = \mathcal{O}\left(t^{-\frac{3}{2}}\right), \tag{50}$$

$$\text{Oseen}\sim a^4\rho_f\hat{t}^{-2} = \mathcal{O}(t^{-2}). \tag{51}$$

Therefore, the Basset drag goes as $t^{-\frac{3}{2}}$ and the Oseen drag as t^{-2}. These scales seem to be valid for $t\sim 1$ to 10 (or for $t\sim 10$ to 100 when $\chi=\mathcal{O}(1)$).

In the sequence, the third characteristic step of the particle motion occurs when it reaches its terminal velocity. In this case, it is clear that $U\sim U_t$. In this last part of the motion, both Basset and Oseen drags have the same temporal behaviours as those presented in Eqs. (48) and (49).

The present analysis also can be used to predict the variations in the temporal evolution of the total force acting on the particle when an inertial convective drag is included in the model. Fig. 7

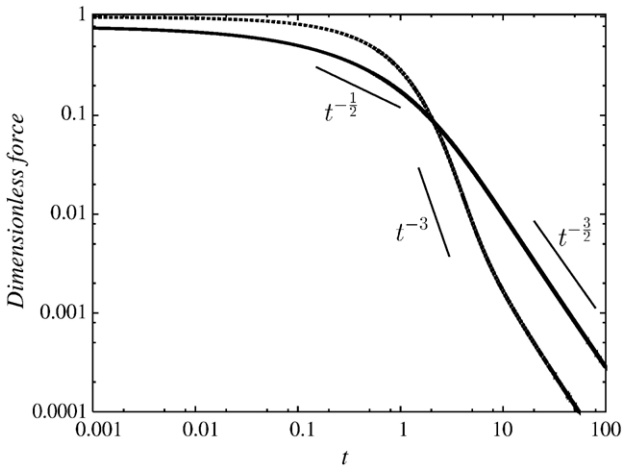

Fig. 7. Evolution of the resultant force acting on the particle for $\chi=1/100$ (dotted line) and for $\chi=1/2$ (solid line) or $Re_s=1/2$.

shows the temporal decay of the resultant force acting on the particle for $\chi=1/100$ and $\chi=1/2$. We can see that for $\chi=1/100$, the initial decay goes like t^{-3} between τ_r up to close to $10\tau_r$. This scale seems to be associated with the balance among the several powers of temporal decays observed in the asymptotic solution of the equation of motion, Eq. (23), and the $\mathcal{O}(t^{-2})$ decay of Oseen's drag and, with a smaller influence, the $\mathcal{O}\left(t^{-\frac{1}{2}}\right)$ of the Basset drag. After this interval, the total force decays like $t^{-\frac{3}{2}}$. In fact, if we analyse Figs. 4 and 7 together, it can be inferred that the t^{-3} decay becomes more important as the Oseen drag starts to dominate the Basset drag, in the interval ranging from 2 to 10 units of dimensionless time. As time evolves, the transient effects of the flow dominate the time-evolution towards the terminal velocity and the $t^{-\frac{3}{2}}$ behaviour, predicted by the scaling given in Eq. (50), is observed. The case $\chi \ll 1$, however, is not of major importance to evaluate the coupling between Basset drag and Oseen drag, as discussed previously.

When $\chi=1/2$, on the other hand, the evolution towards the $t^{-\frac{3}{2}}$ decay is smooth, and a t^{-2} decay is not observed. This is due to the low values of the Oseen drag compared to the Basset drag for times up to $t=50$ (see Fig. 3). Fig. 8, in contrast, shows the decay of the resultant force acting on a particle for different values of Re_s. It is seen that as Re_s increases, a stronger decay of the resultant force occurs after $t=1$ in such a way that for $Re_s=5$ and 10 a decay like t^{-2} clearly exists. For longer times, on the imminence of the steady state, the decay becomes again $t^{-\frac{3}{2}}$. This confirms that the nonlinear inertial mechanisms of the flow do change the order of the temporal decay of the approach to the steady state. Due to the high computational cost to solve Eq. (12) numerically for large time intervals, it was not possible to explore the typical decay rates for very long times, predicted in Eqs. (46) and (47). It might be possible to investigate this long time behaviour based on an asymptotic solution of Eq. (12).

The results presented here, obtained with the traditional kernel of the Basset drag, have shown that the evolution towards the steady state of the motion changes with the presence of inertia. An equally important aspect of the coupling between Basset and Oseen drags is presented in Fig. 8. Note the faster evolution towards the steady state as Re_s increases. For $Re_s=5$, the resultant force acting on the particle is approximately 10 times smaller than the value obtained for $Re_s=1/10$ at t around 100 units of dimensionless time. Therefore, our analysis was able to describe, at least from a qualitative point of view, the faster evolution towards the terminal velocity of the particle when Re_s is not zero.

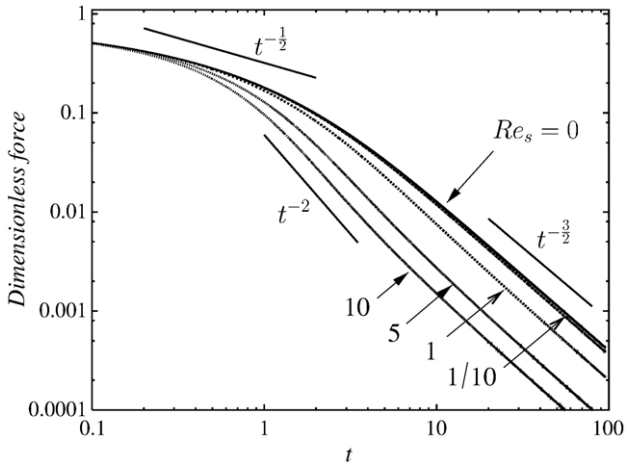

Fig. 8. Evolution of the resultant force acting on the particle for $\chi=1/2$ and for different values of Re_s.

Lawrence and Mei [13] and Coimbra and Rangel [15] have suggested that the form of the convolution kernel is different when the inertia of the flow is considered. Formally, the $t^{-\frac{1}{2}}$-like kernel is valid only for $Re_s=0$. In fact, the $Re_s \to 0$ limit is singular and, for that reason, there ought to be changes in the kernel of the memory integral. An example of different kernels can be found in Lawrence and Mei [13], where they used an asymptotic expression for the Kernel of the memory integral that allowed them to get the predicted theoretical decay of the resultant force on the particle.

While it is true that the effect of the convolution kernel is important to correctly predict the forces acting in a particle, Coimbra and Rangel [23] showed that even though the long-term asymptotic behaviour of the traditional Basset kernel generally overestimates the history force, the use of the traditional kernel has little effect on the velocity and particle position at long times. The reason for the apparent paradox is that the slow, long-term half-power decay of the Basset kernel is only relevant for time scales of the order of the particle relaxation time. Therefore, as Coimbra and Rangel [23] pointed out, the Basset force kernel is incorrect for long times, but the effect of the incorrect kernel at long times is minimised because the steady Stokes drag dominates the forces acting on the particle beyond one relaxation time (see, for instance, Fig. 4 of the present work and, e.g. Coimbra and Rangel [23,24]). This has been more recently validated by experiments performed for a wide range of parameters in Coimbra et al. [25].

When the nonlinear convective effects are concerned, there is still the open question of the determination of the onset of these effects in the motion of particles in the range of small, but nonzero Reynolds numbers. The works of Mei [26] and Lawrence and Mei [13] pointed out that the history drag has a much stronger decay for Reynolds numbers deviating from zero (note that this was not observed in our results, presented in Fig. 6, since we used the standard Basset kernel; we could only observe a reduction on its value after the relaxation time). Therefore, it seems reasonable that the traditional history kernel can be safely used in particle motion calculations where a pseudo-steady force of higher order than the Stokes steady drag is employed. This is because the long-tail asymptotic Basset drag force is less important when convective effects are considered. Both the theoretical and the experimental works available in the literature agree that the short-term behaviour of the traditional Basset drag is correct even for particle Reynolds number larger than unity, as long as the product Reynolds number–Strouhal number is high (for short times or for high frequency flows).

5. Closing remarks

The study of the transient motion of a spherical particle developed in this work has provided insights that are important for modelling two-phase particulate systems. As discussed previously, the mechanisms of transient diffusion of vorticity brought up to the model by the Basset drag are of major importance in the description of the motion of particles whose inertia is comparable to the inertia of the fluid. In particulate systems in which the inertia of the fluid is considerably smaller than the inertia of the particles (as typically occurs in gas–solid suspensions), the unsteady drags can be neglected with no relevant consequences to a correct prediction of the dynamics of these systems. However, the derivation of a model for particulate flows considering such effects is still an open problem and needs further research.

Acknowledgements

The authors gratefully acknowledge the support of CAPES-Brazil, CNPq-Brazil and FINATEC-Universidade de Brasília during the development of this work. We also thank G.C. Abade for the assistance with the numerical calculations, C.F.M. Coimbra and the referees for very insightful and stimulating comments.

Appendix A

The subtraction of the singularity avoids the unbounded growth of numerical errors when a singular, but convergent expression must be evaluated numerically. Specifically, in the present work, the integral

$$I = \int_0^t \left(\frac{\mathrm{d}v}{\mathrm{d}t}\right)_{t=\zeta} \frac{1}{\sqrt{t-\zeta}}\,\mathrm{d}\zeta \tag{52}$$

must be calculated. In the limit of $\zeta \to t$, one has a singularity of type constant/0. In order to avoid this condition, the following procedure is used. Let us to consider the integral I and add to it two integrals with zero sum:

$$I = \int_0^t \left(\frac{\mathrm{d}v}{\mathrm{d}t}\right)_{t=\zeta} \frac{1}{\sqrt{t-\zeta}}\,\mathrm{d}\zeta \underbrace{- \int_0^t \left(\frac{\mathrm{d}v}{\mathrm{d}t}\right)_{t=t} \frac{1}{\sqrt{t-\zeta}}\,\mathrm{d}\zeta + \int_0^t \left(\frac{\mathrm{d}v}{\mathrm{d}t}\right)_{t=t} \frac{1}{\sqrt{t-\zeta}}\,\mathrm{d}\zeta}_{=0}. \tag{53}$$

Note that the term $(\mathrm{d}v/\mathrm{d}t)_{t=t}$ is not a function of ζ, and therefore Eq. (53) can be conveniently rewritten as:

$$I = \int_0^t \left[\left(\frac{\mathrm{d}v}{\mathrm{d}t}\right)_{t=\zeta} - \left(\frac{\mathrm{d}v}{\mathrm{d}t}\right)_{t=t}\right] \frac{1}{\sqrt{t-\zeta}}\,\mathrm{d}\zeta + \left(\frac{\mathrm{d}v}{\mathrm{d}t}\right)_{t=t} \int_0^t \frac{1}{\sqrt{t-\zeta}}\,\mathrm{d}\zeta, \tag{54}$$

where the second integral in Eq. (54) can be calculated analytically. Finally, the convolution integral in Eq. (52) is replaced by

$$I = \int_0^t \left[\left(\frac{\mathrm{d}v}{\mathrm{d}t}\right)_{t=\zeta} - \left(\frac{\mathrm{d}v}{\mathrm{d}t}\right)_{t=t}\right] \frac{1}{\sqrt{t-\zeta}}\,\mathrm{d}\zeta + 2\sqrt{t}\left(\frac{\mathrm{d}v}{\mathrm{d}t}\right)_{t=t}. \tag{55}$$

The integral in Eq. (55) is also singular. However, the singular form 0/0 leads to an accurate numerical evaluation of the integral by the standard methods available in literature [22].

References

[1] T.B. Anderson, R. Jackson, A fluid mechanical description of fluidized beds: equations of motion, I and EC Fundamentals 6 (1967) 527.
[2] Y.D. Sobral, Hydrodynamic and Magnetic Stability of Fluidised Beds, M.Sc. Dissertation DM-73, Department of Mechanical Engineering, University of Brasília, 286p (in Portuguese).
[3] Y.D. Sobral, F.R. Cunha, Hydrodynamic and magnetic effects on the stabilization of concentration waves in fluidized beds, Revista Iberoamericana de Ingeniería Mecánica 9 (1) (2005) 23.
[4] G.G. Stokes, On the effect of the internal friction of fluid on the motion of pendulums, Transactions of the Cambridge Philosophical Society 9 (1851) 8.
[5] C.W. Oseen, Über die Stokessche Formel und über die verwandte Aufgabe in der Hydrodynamik, Arkiv för Matematik, Astronomi och Fysik 6 (No. 29) (1910).
[6] A.B. Basset, A Treatise on Hydrodynamics, Deighton Bell, Cambridge, United Kingdom, 1888.
[7] M.W. Reeks, S. McKee, The dispersive effects of Basset history forces on particle motion in a turbulent flow, Physics of Fluids 27 (7) (1984) 1573.
[8] P.J. Thomas, On the influence of the Basset history force on the motion of a particle through a fluid, Physics of Fluids 4 (9) (1992) 2090.
[9] P.M. Lovalenti, J.F. Brady, The hydrodynamic force on a rigid particle under going arbitrary time-dependent motion at small Reynolds number, Journal of Fluid Mechanics 256 (1993) 561.
[10] I. Proudman, J.R.A. Pearson, Expansions at small Reynolds number for the flow past a sphere and circular cylinder, Journal of Fluid Mechanics 2 (1957) 237.
[11] T. Sano, Unsteady flow past a sphere at low Reynolds number, Journal of Fluid Mechanics 112 (1981) 433.
[12] S. Kim, S.J. Karilla, Microhydrodynamics: Principles and Selected Applications, Butterworth-Heinemann, Boston, USA, 1991.
[13] C.J. Lawrence, R. Mei, Long-time behavior of the drag on a body in impulsive motion, Journal of Fluid Mechanics 283 (1995) 301.
[14] M.R. Maxey, J.J. Riley, Equation of motion for a small rigid sphere in a nonuniform flow, Physics of Fluids 26 (1983) 883.
[15] C.F.M. Coimbra, R.H. Rangel, General solution of the particle momentum equation in unsteady Stokes flow, Journal of Fluid Mechanics 370 (1998) 53.
[16] R.H. Thomas, K. Walters, The unsteady motion of a sphere in an elastico-viscous liquid, Rheologica Acta 5 (1) (1966) 23.
[17] M.T. Matthews, J.M. Hill, Flow around nanospheres and nanocylinders, The Quarterly Journal of Mechanics and Applied Mathematics 59 (2) (2006) 191.
[18] G.K. Batchelor, An Introduction to Fluid Dynamics, Cambridge University Press, Cambridge, United Kingdom, 1967.
[19] L.D. Landau, E. Lifchitz, Mécanique des Fluides, Éditions MIR-Ellipses, Poitiers, France, 1971.
[20] A. Belmonte, J. Jacobsen, A. Jayaraman, Monotone solutions of a nonautonomous differential equation for a sedimenting sphere, Electronic Journal of Differential Equations 62 (2001) 1.
[21] M. Abramowitz, I.A. Stegun, Handbook of Mathematical Functions, Dover Publications, New York, USA, 1974.

[22] W.H. Press, S.A. Teukolsky, W.T. Vetterling, B.P. Flannery, Numerical Recipes in Fortran 77, Second Edition, Cambridge University Press, Cambridge, United Kingdom, 1992.
[23] C.F.M. Coimbra, R.H. Rangel, Spherical particle motion in harmonic Stokes flows AIAA Journal 39 (9) (2001) 1673.
[24] L.E.S. Ramirez, E.A. Lim, C.F.M. Coimbra, M.H. Kobayashi, On the dynamics of a spherical scaffold in rotating wall bioreactors, Biotechnology and Bioengineering 84 (3) (2003) 382.
[25] C.F.M. Coimbra, D. L'Esperance, R.A. Lambert, J.D. Trolinger, R.H. Rangel, An experimental study on stationary history effects in high-frequency Stokes flows, Journal of Fluid Mechanics 504 (2004) 353.
[26] R. Mei, Flow due to an oscillating sphere and an expression for unsteady drag on the sphere at finite Reynolds number, Journal of Fluid Mechanics 270 (1994) 133.